

Dangers of using global bioclimatic datasets for ecological niche modeling. Limitations for future climate projections

Joaquín Bedia^{a,1,*}, Sixto Herrera^b, Jose Manuel Gutiérrez^a

^a*Instituto de Física de Cantabria, Universidad de Cantabria-CSIC. 39005 Santander, Spain*

^b*Predictia Intelligent Data Solutions, S.L. CDTUC Fase A, Planta 2–203. Avda. los Castros s/n 39005 Santander, Spain*

Abstract

Global bioclimatic datasets are being widely used in ecological research to estimate the potential distribution of species using Climate Envelope Models (CEMs). These datasets are easily available and offer high resolution information for all land areas globally. However, they have not been tested rigorously in smaller regions, and their use in regional CEM studies may pose problems derived from their poor representation of local climate features. Moreover, these problems may be enhanced when using CEMs for future climate projections —a topic of current active research,— due to the uncertainty derived from the future altered climate scenarios.

In this paper we use distributional data of European beech (*Fagus sylvatica*) in Northern Iberian Peninsula to analyze the discrepancies of the

*Corresponding author

Email addresses: joaquin.bedia@unican.es (Joaquín Bedia), sixto@predictia.es (Sixto Herrera), gutierjm@unican.es (Jose Manuel Gutiérrez)

¹Instituto de Física de Cantabria, Universidad de Cantabria-CSIC. Facultad de Ciencias, Avda. de los Castros 44 (Room 1068). 39005 Santander, Spain. Tel: (+34)942202064, Fax: (+34)942200935

CEMs (predictive skill, variable importance and consistency using different predictor subsets) resulting from three alternative public, high-resolution climate datasets: A benchmarking regional climate dataset developed for the area of study (UC), the University of Barcelona Atlas for the Iberian Peninsula (UAB) and the worldwide WorldClim bioclimatic dataset (WC). The same CEM techniques (multiple logistic regression and multivariate adaptive regression splines) were applied to the different datasets, showing that the quality of the baseline climate has a great impact on the resulting models, as manifested by the different contributions of the bioclimatic predictors to the resulting models. Artifactual bioclimatic variables were found in some datasets, representing topographical features and spatial gradients, rather than true climatic patterns, thus significantly contributing to the models, although not for the right reasons. This causes a misleading model interpretation and problems for extrapolation in future climate conditions, as evidenced analyzing the future projections obtained using state-of-the-art regional climate projections from the ENSEMBLES project.

Keywords: Species distribution models, WorldClim, UAB Atlas, regional climate projection, impacts of climate change

1. Introduction

Climate Envelope Models (CEMs), also referred to as ecological niche models or species distribution models, are statistical predictive tools applied in ecological research to estimate the distribution of species, biological communities or habitats (Guisan and Zimmermann, 2000; Elith and Leathwick, 2009). The use of these models is widespread throughout the ecological litera-

7 ture in a variety of application fields, such as biodiversity conservation (Wilt-
8 ing et al., 2010), invasive species propagation (Jeschke and Strayer, 2008) and
9 impacts of climate change (Thuiller, 2003; Araújo et al., 2005), among others.
10 Typically, these techniques use medium to high-resolution grids (several min-
11 utes to seconds of arc, see e.g. Kriticos et al., 2012) over the area of interest
12 and combine observations of species occurrence with appropriate bioclimatic
13 indicators defined at the grid box scale. The result is a predictive model
14 assigning a probability of occurrence to each of the grid boxes as a function
15 of the bioclimatic indicators.

16 The recent development of new global high-resolution bioclimatic datasets
17 has broaden the scope of CEMs across different regions and continents and
18 has also boosted their application in climate change impact studies (Peterson
19 et al., 2002; Hijmans and Graham, 2006). The need for high-resolution input
20 data in this context has been already highlighted by some authors, given the
21 inability of coarse-resolution models to represent local refugia (e.g. Randin
22 et al., 2009; Franklin et al., 2013). One of the most popular global bioclimatic
23 products is the WorldClim dataset (Hijmans et al., 2005), which is widely
24 being used because it is easily available and offers high resolution ($\sim 1\text{km}$) for
25 all land areas globally. Other newer global interpolated products of similar
26 characteristics have appeared recently in the literature (e.g. the new Climond
27 dataset, Kriticos et al., 2012, which is partly based on WorldClim data),
28 indicating the high demand of these kind of products in the last years.

29 However, these global datasets have not been tested rigorously in smaller
30 regions, and their use in regional studies may pose problems derived from
31 their poor representation of local climate features over certain areas. To

32 date, most of the studies fail to explicitly analyze the sensitivity of CEMs to
33 the baseline climate data (Peterson and Nakazawa, 2008; Soria-Auza et al.,
34 2010), partly because of the lack of high-quality climate datasets—in many
35 areas of the world—that may be confidently used as a reference. Moreover,
36 in those studies applying CEMs for future climate projections, the defects of
37 the baseline climatology may be enhanced by the uncertainty derived from
38 the future climate scenarios (Beaumont et al., 2008; Wiens et al., 2009), thus
39 seriously compromising the practical validity of the resulting projections for
40 planners and adaption-strategists (see, e.g., Araújo and New, 2006).

41 In this study we present a sensitivity analysis of CEMs to different base-
42 line climate datasets, using distributional data of a tree species—the Eu-
43 ropean Beech (*Fagus sylvatica* L.), *Fagus* henceforth—in Northern Iberian
44 Peninsula. In particular, we consider three different climate datasets encom-
45 passing a range of spatial extents, from global to regional: The WorldClim
46 global database, the Atlas by the Universitat Autònoma de Barcelona for the
47 Iberian Peninsula (Ninyerola et al., 2005), and the benchmark high-quality
48 regional grid developed by the authors at the University of Cantabria for the
49 region of study (Gutiérrez et al., 2010); hereafter we will refer to them as
50 WC, UAB and UC respectively. The same CEM techniques (multiple logistic
51 regression and multivariate adaptive regression splines) were applied to the
52 different datasets, evaluating the resulting models in the light of their AUC
53 and Cohen’s κ , as the usual performance metrics in CEM studies.

54 A first comparison of the three datasets reveals deficiencies of WorldClim,
55 which fails to properly represent all precipitation bioclimate indices over
56 the region. We show how these artifactual indices are actually representing

57 topographical features and spatial gradients as a result of the underlying
58 interpolation process, rather than true climatic patterns, thus significantly
59 contributing to the CEM models, although not for the right reasons. This
60 causes a misleading interpretation of the resulting models and problems for
61 extrapolation in future climate conditions. The problems found are beyond
62 the deficiencies reported for WorldClim precipitation in mountainous areas
63 (Hijmans et al., 2005; Tadić, 2010).

64 In order to estimate the sensitivity of the resulting CEMs in future cli-
65 mate scenarios, we considered the regional projections given by the ensem-
66 ble of Regional Climate Models (RCMs) from the EU-funded ENSEMBLES
67 project for the A1B scenario (Jacob et al., 2007). First, the *delta* method
68 was applied to obtain the future climate projections —and the correspond-
69 ing derived bioclimatic indices,— adding the differences to the three different
70 baseline climatologies (see, e.g., Räisänen, 2007; Zahn and von Storch, 2010,
71 for a description and application of delta method). Then, future projections
72 of species distributions were obtained by applying the different CEM models
73 to the corresponding future bioclimatic indices. The resulting projections dif-
74 fered markedly —particularly for WorldClim,— highlighting the inadequacy
75 of high resolution worldwide climate datasets for their application in regional
76 climate change studies. However, when only temperature-related bioclimatic
77 variables —more robust across the different datasets— were included, the
78 projections were in relatively good agreement for all the datasets.

79 This paper is organized as follows. In Sec. 2 the area of study and datasets
80 used in the paper are presented. Sec. 3 describe the different methodologies
81 applied, including CEM modeling algorithms, model assessment. The main

82 results and discussion are presented in Sec. 4. Finally, some conclusions are
83 given in Sec. 5.

84 2. Area of Study and Datasets

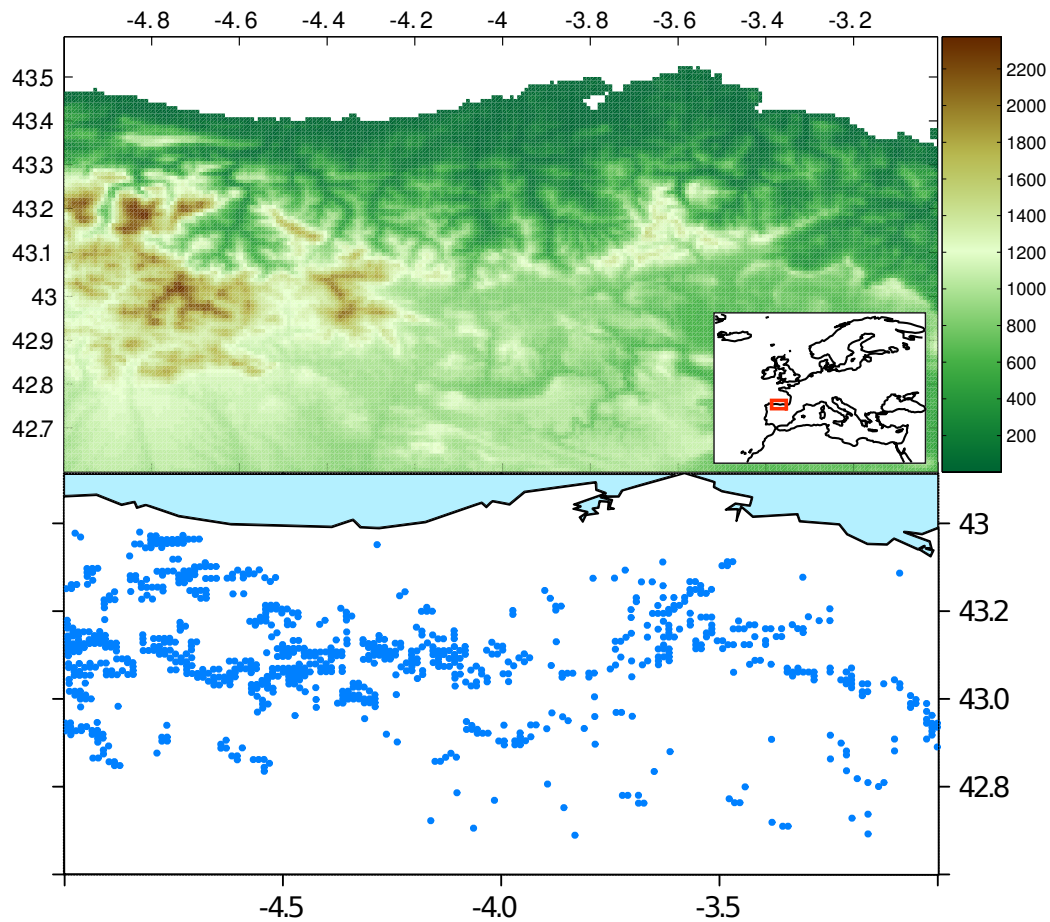


Figure 1: Location of the study area. In the top panel the orography of the target area is represented at a 1km resolution (meters above sea level). In the lower panel, the distribution of *Fagus* is shown at a 1km pixel resolution.

85 The area of analysis in this study is centered in Northern Iberian Penin-

86 sula, with a bounding box of coordinates $42.60^{\circ}N$, $-5.00^{\circ}E$ to $43.60^{\circ}N$, $-2.99^{\circ}E$
87 (Fig. 1). In the Iberian Peninsula, *Fagus* forests are mainly found in the
88 Northern mountain areas although they reach the Iberian and Central Ranges
89 at some particular locations (Costa et al., 1998). *Fagus* has a restricted niche
90 in the study area, linked to mountainous areas mostly between 400 and 1400m
91 above sea level. 95% of the presence localities used in this study lie within
92 this elevation range, showing a very clear unimodal distribution. The sharp
93 interaction between *Fagus* and the climatic gradient in the study area has
94 motivated the choice of this species, which is expected to be modeled with
95 higher accuracy than other generalist species (Brotons et al., 2004; Araújo
96 and Guisan, 2006; Tsoar et al., 2007). This region is determined by the ex-
97 tent of the UC climate grid, which has the smallest geographical extent of
98 the datasets used in this study.

99 *2.1. Species distribution data*

100 The information on *Fagus* distribution was obtained from the Forest Map
101 produced by the Third National Forest Inventory (MARM, 2006). The origi-
102 nal vector map was filtered so that all polygons containing the target species
103 were retained and then rasterized to a pixel size of 0.0083° (aprox. 1km),
104 leading to a total of *ca.* 900 localities of presence within the study area
105 (Fig. 1, bottom panel).

106 Most probabilistic modeling methods require absence points—in addi-
107 tion to occurrences—for training (see e.g. Bedia et al., 2011). Since we
108 lacked of real absences, we generated synthetic background points assigning
109 them a value of zero (absence). Occurrence data define the conditions un-
110 der which the species is more likely to be present, whereas background data

111 establishes the environmental domain of the study (Hijmans et al., 2012).
112 Thus, background points do not represent actual absences, and they are ran-
113 domly generated in an equal number to the presences, following some authors
114 who suggest that intermediate prevalences produce better results (McPher-
115 son et al., 2004; Allouche et al., 2006; Mateo et al., 2010). In addition, we
116 set a buffer radius of 2000m around known presences, in order to minimize
117 false negatives due to cartographic inaccuracies inherent to the delineation
118 of vectorial maps (Graham et al., 2008).

119 *2.2. Baseline climate datasets*

120 For the sake of conciseness, we only introduce their main characteristics
121 of the climate datasets used in this study, with some emphasis in the descrip-
122 tion of the more recent benchmarking UC dataset. The interested reader is
123 referred to the published documentation of these datasets for further details
124 on their construction.

125 WorldClim (WC, Hijmans et al., 2005) is a global temperature and pre-
126 cipitation dataset with a spatial resolution of 30 arc-seconds (aprox. 1km),
127 obtained applying a thin-plate spline smoothing interpolation algorithm to
128 a large number of weather stations throughout the world, covering most of
129 Earth’s for approximately 50 years (1950–2000). This dataset is freely avail-
130 able for download from internet (<http://www.worldclim.org>).

131 The climate surfaces of the University of Barcelona Atlas (UAB, Ninyerola
132 et al., 2005) were calculated by multiple regression and residual analysis,
133 introducing as covariates a relatively simple set of variables: altitude, slope,
134 different indices used to describe distance to the sea, solar radiation and
135 terrain curvature. Temperature and precipitation data for the period 1950–

136 2000 were obtained from the national network of the Spanish Meteorology
137 Agency (AEMET), and from the literature in the case of Portugal. The
138 UAB dataset is provided at a very high resolution (200m) for the entire
139 Iberian Peninsula, and is available for download from the internet (<http://opengis.uab.es/wms/iberia/mms/index.htm>).
140

141 The high resolution climate grid developed for Cantabria and surround-
142 ing territories by the University of Cantabria (UC, Gutiérrez et al., 2010),
143 is based on the same AEMET stations network than UAB. Data from 148
144 (62) stations were used for precipitation (temperature), respectively, after a
145 process of data quality control, within the period 1950-2003. All data series
146 were required to have a minimum of 10 years with less than 10% of miss-
147 ing values, and they were tested for relative homogeneity (Alexandersson,
148 1986; Alexandersson and Moberg, 1997) and absolute homogeneity (SNHT
149 method, Khaliq and Ouarda, 2007), after discarding outliers. The perfor-
150 mance of different techniques was tested, namely thin-plate splines, angular
151 distance weighting and kriging (Kriging, 1951), obtaining best results with the
152 latter one. This method has been widely used in climate research (Atkinson
153 and Lloyd, 1998; Biau et al., 1999; Haylock et al., 2008) and provides high
154 flexibility for covariate introduction and uncertainty analysis. In the case
155 of the precipitation, a two-step interpolation process was conducted: first,
156 precipitation occurrence was interpolated using *indicator kriging* (Juang and
157 Lee, 1998); then, the amount of precipitation was interpolated using ordinary
158 kriging, assigning values of 0 to all ‘dry’ points. Thus, the frequency distri-
159 bution of precipitation for both occurrence and amount was optimally fit.
160 In the calculation of uncertainty, the dependency among observations was

161 incorporated following Yamamoto (2000). The final 1km-resolution grid was
162 obtained by regression-kriging (Hengl et al., 2007), introducing a set of ba-
163 sic covariates describing terrain characteristics including, elevation, distance
164 to coastline, and topographic blocking effects. The interpolated tempera-
165 ture and precipitation were subject to expert revision by meteorologists of
166 AEMET based on their deep knowledge on the climate of this region (Cano,
167 1999), leading to final refinement by elimination of some coastal weather sta-
168 tions with systematic errors, not detected in the previous stage of automated
169 data quality control.

170 Thus, UC and UAB are constructed upon the same network of stations
171 and using a similar methodology, based on multiple linear regression with
172 a residual adjustment by means of an interpolation process. The main dif-
173 ferences between them lie the level of detail at which the resulting surfaces
174 have been checked for quality, due to their different geographical coverages,
175 and in the type of covariates introduced into the models. In this sense, UAB
176 uses an input orography of 200m resolution, and introduces terrain curva-
177 ture among other covariates, thus leading to a fine-grain level of detail that
178 is then propagated into the climate surface by the regression model. On the
179 other hand, WC is based on thin-plate splines, considering a simple set of
180 covariates (longitude, latitude and elevation), which are applied to a much
181 more sparse network of observations, provided its worldwide coverage.

182 In this work we consider the set of 19 bioclimatic indices provided by
183 WorldClim, which are commonly used in ecological modeling (see Table 1).
184 To allow for full spatial comparability among the three datasets (UC, UAB
185 and WC), the original layers were re-projected to geographical coordinates

186 and resampled to match the same 1km regular grid. For UC and UAB,
187 the bioclimatic indices were derived from the precipitation and temperature
188 layers provided in those cases. The common baseline period 1950–2000 was
189 selected for the three datasets based on their temporal overlapping. The
190 resulting bioclimatic indices are compared in Table 1 and partially displayed
191 in Fig. 3.

192 *2.3. Future climate projections*

193 In order to calculate future projections of species distributions using
194 CEMs, we considered the state-of-the-art regional projections given by seven
195 Regional Climate Models (RCMs, Table 2) from the EU-funded ENSEM-
196 BLES project (van der Linden and Mitchell, 2009). These RCMs were run
197 over a limited domain covering Europe with a horizontal resolution of 25km,
198 driven at the boundaries by different GCM simulations under the A1B emis-
199 sion scenario (Nakićenović, 2000). However, it has been recently recognized
200 that the outputs of the RCMs cannot be used directly for impact studies,
201 since they may contain important biases resulting from different physics and
202 parameterizations involved in their formulation (Winkler et al., 1997). To
203 alleviate this problem, we applied the so-called ‘delta’ method (see, e.g.,
204 Räisänen, 2007; Zahn and von Storch, 2010) or ‘change factors’ (Winkler
205 et al., 1997) and, thus, the baseline climatological values are modified at
206 a grid-box level by a change factor, obtained as the difference/ratio of the
207 temperature/precipitation values between a future period (e.g. 2071-2100)
208 and the control period (1970-1999 in this study). We computed the altered
209 future bioclimatic indices for the periods 2011–2040, 2041–2070 and 2071–
210 2100, based on the climate change signals for precipitation, minimum and

211 maximum temperature values. The mean ensemble increments (and devia-
212 tions) obtained for the region of study for the periods 2011–2040, 2041–2070
213 and 2071–2100 were, respectively, -32.2 (47.6), -93.8 (32.2) and -173.3 (82.5)
214 mm/year for precipitation; 0.80 (0.18), 1.76 (0.19) and 2.54 (0.12) °C for
215 minimum temperature, and 0.92 (0.17), 1.98 (0.14) and 2.94 (0.22) °C for
216 maximum temperature.

217 **3. Methods**

218 *3.1. CEM modeling algorithms*

219 CEMs were originally constructed using a number of probabilistic al-
220 gorithms, namely generalized linear models, support vector machines, artifi-
221 cial neural networks, maximum entropy, and multivariate adaptive regression
222 splines (see Bedia et al., 2011, for a comparative analysis of this techniques
223 in the framework of species distribution modeling). All methods yielded sim-
224 ilar results, with slight to moderate differences in the resulting probabilistic
225 distributions, leading to the same overall conclusions. We selected gener-
226 alized linear models (GLMs) as the preferred technique to use, given that
227 the focus of this study is to analyze the uncertainties derived from the base-
228 line climatology, rather than the inherent differences stemming from the use
229 of different modeling algorithms. Although non-linear techniques may lead
230 to models of improved predictive accuracy (Elith et al., 2006; Bedia et al.,
231 2011), on the other hand they may eventually obscure the actual contribu-
232 tion of each variable proven their higher complexity. With this regard, GLMs
233 provide a flexible and robust framework for assessing the statistical signif-
234 icance of the explanatory variables and the estimation of their importance

235 (see Section 3.4), providing a simple and sound model interpretability at a
236 low computational cost (see Guisan et al., 2002, for an overview of GLMs in
237 the context of species distribution modeling). Nevertheless, throughout the
238 manuscript we will also present some results corresponding to the Multivari-
239 ate Adaptive Regression Splines models (MARS, Friedman, 1991) as an ex-
240 ample of non-linear technique, that illustrates the consistency of the results
241 regardless of the modeling technique applied. MARS is a non-parametric
242 method for regression which approximates the underlying function through
243 a set of adaptive piecewise linear regressions, known as *basis functions*. More
244 details on this method are presented in (Bedia et al., 2011).

245 3.2. Correlation analysis

246 The high inter-dependence between some of the bioclimatic variables used
247 as predictors (Table 1) gives raise to the issues of redundancy and multi-
248 collinearity, negatively affecting variable selection and model interpretability
249 due to the drastic changes in model parameter values, and also hampering
250 the ability of the model for extrapolation (Brauner and Shacham, 1998), cen-
251 tral in climate change studies. In order to avoid redundancy, we eliminated
252 from the analysis the bioclimatic variables yielding correlation values above
253 0.95 (Spearman's rho coefficient) in the pairwise cross-correlation matrix of
254 each dataset (*intra-dataset* correlations). The threshold of 0.95 is conser-
255 vative, and it was chosen in order to keep other variables that, although
256 also highly correlated, may still provide some useful additional information.
257 Moreover, in the next step, collinear variables have been set aside of subse-
258 quent analyses (Sec 3.3). In addition, we also computed pairwise correlations
259 between datasets (*inter-dataset* correlations) as a first exploratory analysis

260 of the consistency of the different climatologies.

261 *3.3. Multicollinearity analysis and variable selection*

262 After the elimination of highly correlated variables, the resulting non-
263 redundant datasets were further checked for multicollinearity. Among the
264 different approaches available for detecting multicollinearity (see Brauner
265 and Shacham, 1998, for an overview), we have followed the classical method
266 based on the condition number of the normal matrix, which has been exten-
267 sively used for collinearity diagnosis (Brauner and Shacham, 1998). In the
268 absence of multicollinearity, the eigenvalues, condition indices and condition
269 number of the predictors matrix will all equal one. As collinearity increases,
270 eigenvalues will be both greater and smaller than one (eigenvalues close to
271 zero indicate a multicollinearity problem), and the condition indices and the
272 condition number will increase, leading to an unstable model definition.

273 The simplest approach to circumvent multicollinearity consists of drop-
274 ping all collinear variables. However, in order to avoid inferential problems
275 derived from arbitrarily dropping/retaining predictors (Graham, 2003), we
276 have followed a sequential data-driven modeling approach: first, the variable
277 attaining the highest predictive performance (in terms of AUC) is retained.
278 Then, the remaining variables are tested for collinearity, setting a maximum
279 allowable condition number below 30. Those variables producing condition
280 numbers above the threshold of 30 are dropped, and the selection proce-
281 dure is iteratively repeated until no more candidate variables remain. The
282 main disadvantage of this approach is that no critical value for the condi-
283 tion number has been established to indicate harmful collinearity (Brauner
284 and Shacham, 1998). The value chosen has been suggested by (Cohen et al.,

285 2003), and represents a “rule of thumb” criterion, that we deemed appro-
 286 priate in this case after checking the the low cross-correlation values of the
 287 resulting datasets (Fig.2) and their spatial distribution (Fig.3). We followed
 288 this variable selection procedure for each dataset (UC, AUB and WC) lead-
 289 ing to three different sets of bioclimatic predictors, subsequently used in the
 290 following analyses.

291 3.4. Variable importance assessment

292 In order to estimate variable importance in the context of logistic regres-
 293 sion, we have applied the method of hierarchical partitioning, by which the
 294 independent effect of each variable is calculated by comparing the fit of all
 295 models containing a particular variable to the fit of all nested models lacking
 296 that variable (Chevan and Sutherland, 1991). For instance, for variable X_1 ,
 297 its importance I would be calculated as follows:

$$I_{x1} = \sum_{i=0}^{k-1} \frac{\sum (r_{y, X_1 X_h}^2 - r_{y, X_h}^2) / \binom{k-1}{i}}{k} \quad (1)$$

298 where X_h is any subset of i predictors from which X_1 is excluded. As a result,
 299 the variance shared by two or more correlated predictors can be partitioned
 300 into the variance attributable to each predictor. This method provides a
 301 robust assessment of variable importance and has been shown to outper-
 302 form other methods used for variable importance estimation in the context
 303 of regression analysis, after the removal of spurious variables (Murray and
 304 Conner, 2009).

305 3.5. Model assessment

306 We performed a k -fold cross-validation of the models, with $k=10$ stratified
307 randomly splitted subsets of presence/absence, each of them containing an
308 approximately equal number of presences and absences (50%), following the
309 criteria presented in Section 2.1. Model skill was assessed by computing the
310 ROC curves for each model and calculating the corresponding AUCs. We
311 also computed Cohen's κ using prevalence as the probability cutoff threshold
312 ($P = 0.5$).

313 All the analyses were conducted in the R language and environment for
314 statistical computing (R Development Core Team, 2012).

315 4. Results and Discussion

316 4.1. Correlation analysis of bioclimatic variables

317 The intra-dataset pairwise correlation analysis identified some redundant
318 variables, common to the three datasets (Fig. 2a-b). As a result, BIO1, 6
319 and 11, based on temperature data, were in all cases highly cross-correlated
320 ($\rho > 0.95$), and only BIO11 was retained. Regarding precipitation, variables
321 BIO12 and 13 (redundant with BIO16) and BIO17 (redundant with BIO14)
322 were dropped for the same reason. There is a high number of temperature-
323 related bioclimatic variables highly correlated with precipitation ones in the
324 WC dataset, whereas these correlations are lower and less frequent in the case
325 of UAB and UC. As an example, unlike UC and UAB, BIO5 of WC shows
326 a very high correlation with BIO14 and BIO17 (Fig. 2b). This constitutes a
327 first note of warning on the problems with the precipitation variables in WC.

328 The inter-dataset pairwise correlations revealed remarkable differences
329 between the bioclimatic variables among datasets. The lack of consistency
330 between datasets is more accentuated for WC than for UAB, with regard to
331 the UC data (Fig. 2c-d). There is a general good agreement between precip-
332 itation variables of UAB and UC, but there is scarce correspondence in the
333 case of WC, highlighting again the problems derived from precipitation data
334 in WC. These differences become apparent in the spatial distribution of the
335 bioclimatic variables displayed in Fig. 3. For instance, BIO14 (precipitation
336 of the driest month) has a comparable spatial distribution for UC and UAB.
337 Although UAB exhibits a fine-grain level of detail that seems not realistic in
338 this case, it does not significantly alter the overall spatial pattern, preserving
339 a high level of agreement with UC ($\rho=0.91$, $rmse=4.8$). On the contrary,
340 BIO14 of WC has a markedly different spatial distribution and magnitude
341 ($\rho=0.64$, $rmse=13.7$). Similar results are obtained for BIO15, which in the
342 case of WC is strongly correlated with the topography, and unlike UC and
343 UAB, with negative sign (Fig. 4). With regard to the temperature-related
344 bioclimatic variables, BIO9 (mean temperature of the driest quarter) is the
345 most similar among datasets, evidencing a close relationship with the orog-
346 raphy in all cases (Fig. 4). On the other hand, BIO3 (isothermality) and
347 BIO5 (maximum temperature of the warmest month), are not correlated at
348 all with orography in UC, but they are in UAB and WC. Moreover, in the
349 case of BIO3, the signs of the correlation of UAB and WC are opposite.

350 Therefore, the correlation analysis revealed important inconsistencies be-
351 tween datasets. The largest deviations are exhibited by WC, with some
352 bioclimatic patterns that seem more related with orography than with the

353 actual climatic features of the study area, as represented by UC. This is spe-
354 cially true in the case of precipitation, as none of the bioclimatic variables is
355 able to approximate the UC and UAB precipitation pattern, which in general
356 terms are more similar than WC. However, regardless of their dependence on
357 temperature or precipitation, the most differing bioclimatologies correspond
358 to those related with climatic variability (BIO2 and 3 for temperature, and
359 BIO15 for precipitation). In this case, UAB also failed to approximate the
360 UC climatologies.

361 *4.2. Variable selection and importance in the models*

362 The large differences among the bioclimatic datasets, with intra-dataset
363 dependencies and correlations of varying nature and magnitude, prevents
364 from the use of a common subset of variables for the development of the
365 CEM models, from which an overall assessment of variable importance can
366 be made. Thus, we applied the variable selection procedure independently to
367 each dataset, which yielded the predictor combinations (or *subsets* hereafter)
368 presented in Table 3.

369 In all cases, the first variables chosen (based on their maximization of
370 model AUC), were related with temperature. These were BIO9 (mean tem-
371 perature of the driest quarter) in the case of UC and WC, and BIO5 (maxi-
372 mum temperature of the warmest month) in the case of UAB, both related
373 with the temperature regime during summer in the study area. In the case
374 of BIO9, due to its strong control by orography (Fig. 4), the differences of
375 UAB and WC with UC are minor. In the case of BIO5, WC shows a 2°C
376 mean bias, although the spatial pattern is well preserved in general terms.
377 Variable BIO14 (Precipitation of the driest month) was included in the three

378 subsets of predictors.

379 For the sake of conciseness, in the analysis of variable importance we
380 will display only the results of the UC subset, provided that the overall
381 results and conclusions are similar when the UAB and WC subsets are used
382 instead. The variable importance given to temperature-related variables is
383 quite high in the case of the UC model, and also in the case of UAB, whereas
384 WC models tend to give larger importance to precipitation-related variables,
385 notably BIO14 (Fig. 5).

386 The variable importance in the models evidences that temperature is an
387 important variable for modeling *Fagus* distribution, which implies a strong
388 orographic component, as highlighted in Fig. 4. Nevertheless, there is an
389 important fraction of the variability explained by precipitation in the UC
390 model (BIO16), a variable that is weakly correlated with the elevation in the
391 study area, and therefore the added value of precipitation for *Fagus* modeling
392 should not be disregarded. As a result, some variables very correlated with
393 topography are very important for *Fagus* CEMs. In the case of precipitation
394 variables of WC, this relationship with the orography is not justified by a
395 real climatic phenomenology, but rather by a side effect of the interpolation
396 algorithm. The same applies to some temperature-related bioclimatic vari-
397 ables, like BIO2 and BIO5, that both UAB and WC include with preference
398 in their models, and which exhibit large differences with the UC benchmark.

399 4.3. Predictive skill of the models

400 For the assessment of CEM predictive skill, we computed the AUC and
401 Cohen's κ of the 10-fold cross validation models, considering for each dataset
402 its own subset of predictors (Table 3), thus maximizing the predictive skill

403 in each case. All models achieved fairly high AUC and Cohen’s κ values,
404 typically attributed to predictive systems with a good discrimination abil-
405 ity (Swets, 1988; Landis and Koch, 1977). The results corresponding to Co-
406 hen’s κ are comparable to those obtained by AUC, and thus, for the sake of
407 brevity, we will refer only to AUC hereafter. In addition, the results achieved
408 by the more sophisticated MARS algorithm are also displayed, evidencing its
409 better performance in terms of AUC (Fig. 6), although in relative terms, the
410 results are similar to GLMs.

411 As previously shown, some precipitation variables have a large weight in
412 the WC model, even though they do not correspond to the actual precipita-
413 tion pattern in the study area. However, this had no apparent effect on the
414 CEM skill, which was similar in the three datasets, with a slightly better per-
415 formance of GLM in the case of UAB (median > 0.90 considering the $k=10$
416 models of the k-fold cross validation. Fig. 6, lower panel). Given that the
417 largest differences between datasets are in precipitation, we also computed
418 CEMs using temperature variables only (indicated in Table 3 without the
419 asterisk). In this case, the results were more similar across datasets, with a
420 very slight loss of skill, more apparent for MARS than for GLM models, prob-
421 ably due to the non-linearities between both types of variables that MARS
422 is able to capture. The inclusion of precipitation improved the predictive
423 skill of the UAB and UC models, confirming the added value of precipitation
424 for *Fagus* modeling, previously indicated in the independent effects analysis
425 (Sec. 4.2). On the contrary, the removal of precipitation variables in the WC
426 model did not produce any changes the AUC, evidencing that precipitation
427 variables of WC provide little or no improvement at all in CEM skill, once

428 temperature-related ones are used.

429 4.4. CEM predictions and uncertainty

430 As it can be expected from the similar predictive skills attained by the
431 UC, UAB and WC *Fagus* CEMs, the probabilistic maps yielded similar re-
432 sults in terms of spatial distribution of *Fagus* potentiality (Fig. 7a), although
433 some fine-grain details, previously shown in the bioclimatic predictors, are
434 now apparent in the predicted distributions of UAB. The sharp transitions
435 between presence and absence in UAB and WC (probability threshold of
436 0.5), contrasts with the smooth probabilistic spatial prediction of the UC
437 model. In order to test the robustness of these models to changes in the
438 predictor combinations, we alternatively constructed CEMs using the three
439 different variable subsets (Table 3) for each climate dataset, and computed
440 the standard deviation of the resulting distribution maps. We found that
441 UC yielded very similar distributions in all cases, whereas the spread of the
442 predictions was larger in the case of UAB and WC (Fig. 7b), showing the
443 robustness of the UC models to changes in the predictor combinations.

444 4.5. Future distribution forecasting

445 Future *Fagus* distributions were computed using the models obtained
446 in the previous section, but driven by the regional scenarios described in
447 Sec. 2.3, calculated according to the delta method. The future distributions
448 corresponding to each RCM projections were computed individually, and
449 the mean and standard deviation of the resulting ensemble was computed
450 in a grid box basis (Fig. 8). Note that in the future maps presented, espe-
451 cially in the case of WC, the native grid of the RCMs is noticeable. This

452 is the “true” resolution of the climate change signal provided by the EN-
453 SEMBLES RCMs ($\sim 25\text{km}$), added to the baseline climatology applying the
454 delta method. Thus, the resulting squared tessellation is not an artifact, but
455 the real resolution at which projections can be realistically provided in this
456 case. We prefer to keep it instead of smoothing the maps by means of an
457 interpolation process, as this would represent an added source of uncertainty
458 to the projections. In addition, by preserving the original resolution of the
459 climate change signal, the spatial consistency of UC and UAB models when
460 deltas are applied is highlighted, as opposite to WC, which also constitutes
461 an indication of the lack of robustness of WorlClim in the representation the
462 climate in the region of analysis.

463 In general, future distributions using UC and UAB datasets are simi-
464 lar, and represent the expected trend of *Fagus* retreat in its southern Eu-
465 ropean limit of distribution, in accordance with previous studies on this
466 species (Kramer et al., 2010; Felicísimo et al., 2010). In contrast, future
467 range projections produced by WC do not follow a logical pattern, in the
468 sense that a very sudden decline in potentiality is projected for the first pe-
469 riod (2011-2040), that is reverted during the second period (2041-2050). In
470 addition, the uncertainty (i.e., the standard deviation of the ensemble) as-
471 sociated to WC projections is very large, a clear symptom of an unreliable
472 future projection.

473 Note, however, that when only temperature-related bioclimatic variables
474 —more robust across the different datasets— are considered in the modeling
475 process, the projections obtained with the resulting CEMs are in relatively
476 good agreement for all the datasets and similar to the full-variable results

477 obtained in the case of UC. This gives some extra evidence of the instability
478 caused in the future projections by the deficiencies of the baseline climate in
479 the CEM modeling process.

480 5. Conclusions

481 We found that the precipitation of WorldClim does not correspond to the
482 actual climatic conditions in the study area, neither in the spatial pattern
483 represented, nor in its magnitude. On the contrary, the UAB dataset was
484 able to preserve both characteristics, although other problems derived from
485 the inclusion of fine-grain covariates in the regression models were noticeable
486 in some bioclimatic maps and in the resulting CEMs. Even though temper-
487 atures had a similar spatial distribution in all datasets –with an important
488 negative bias in the case of maximum temperatures in WC–, some of the
489 derived bioclimatic variables, such as the mean diurnal temperature range
490 and the isothermality, showed large differences. With this regard, our re-
491 sults evidence the reliance of these bioclimatic variables on the orography,
492 attributable to the interpolation methods used to build the climatologies.

493 As a result, in spite of the large differences among datasets and the high
494 importance attained by precipitation-related variables in the WC model,
495 their respective CEMs were able to skillfully predict current *Fagus* distri-
496 bution in all cases, attaining similar model performances after the cross-
497 validation tests, and consistent results independently of the modeling algo-
498 rithm used. Nevertheless, in the case of UAB and WC, this comes at the cost
499 of a misleading model interpretation and a lack of robustness of the resulting
500 CEMs with the introduction of new predictor combinations. With regard to

501 future projections, as far as the climate change signals in the delta method
502 are not added to true climatic features, but on statistical artifacts highly
503 related to the topography, the resulting future maps obtained using WC be-
504 come unreliable due to the large spread of the forecasts, yielding non-robust
505 projections.

506 Modelers should be aware of the limitations imposed by the poor repre-
507 sentation of regional climate that global datasets perform at some areas of
508 the world. Due to the lack of adequate high-resolution data for validation in
509 many areas of the world, the problems derived from the use of WorldClim for
510 CEM development at a regional/local scale might not be readily apparent,
511 given that model skill, as determined by the commonly applied performance
512 metrics, is not necessarily as bad as to discard the models. However, we
513 warn about the potentially misleading interpretability of the resulting mod-
514 els and their inadequacy for climate change studies, which seriously impair
515 their practical applicability in biodiversity management and conservation
516 planning.

517 Finally, we want to emphasize that the aim of this study is to warn about
518 the critical importance of accurate input climate data for CEM analysis and
519 interpretability, and subsequent extrapolation to future climate conditions,
520 and not the estimation of the current/future bioclimatic potentiality of *Fagus*,
521 that would require accounting for other sources of uncertainty beyond the
522 scope of this paper (see, e.g. Fronzek et al., 2011).

523 **6. Acknowledgements**

524 This research has received funding from the European Union’s Seventh
525 Framework Programme under grant agreements 243888 (FUME Project) and
526 from the CICYT project EXTREMBLES (CGL2010-21869). We thank two
527 anonymous reviewers, who provided insightful comments that greatly im-
528 proved the original manuscript.

529 **References**

530 Alexandersson, H., 1986. A homogeneity test applied to precipitation data.
531 J. Climatol. 6, 661–675.

532 Alexandersson, H., Moberg, A., 1997. Homogenization of swedish tempera-
533 ture data. Part I: Homogeneity test for linear trends. Int. J. Climatol. 17,
534 35–54.

535 Allouche, O., Tsoar, A., Kadmon, R., 2006. Assessing the accuracy of species
536 distribution models: prevalence, kappa and the true skill statistic (TSS).
537 J. Appl. Ecol. 43, 1223–1232.

538 Araújo, M.B., Guisan, A., 2006. Five (or so) challenges for species distribu-
539 tion modelling. J. Biogeogr. 33, 1677–1688.

540 Araújo, M.B., New, M., 2006. Ensemble forecasting of species distributions.
541 Trends Ecol. Evol. 22, 42–47.

542 Araújo, M.B., Pearson, R.G., Thuiller, W., Erhard, M., 2005. Validation of
543 species-climate impact models under climate change. Glob. Change Biol.
544 11, 1504–1513.

- 545 Atkinson, M., Lloyd, C.D., 1998. Mapping precipitation in Switzerland with
546 ordinary and indicator kriging. *Journal of Geographic Information and*
547 *Decision Analysis* 2, 65–76.
- 548 Beaumont, L.J., Hughes, L., Pitman, A.J., 2008. Why is the choice of future
549 climate scenarios for species distribution modelling important? *Ecology*
550 *Letters* 11, 1135–1146.
- 551 Bedia, J., Busqué, J., Gutiérrez, J.M., 2011. Predicting plant species dis-
552 tribution across an alpine rangeland in northern Spain: a comparison of
553 probabilistic methods. *Applied Vegetation Science* 14, 415–432.
- 554 Biau, G., Zorita, E., von Storch, H., Wackernagel, H., 1999. Estimation of
555 precipitation by kriging in the EOF space of the sea level pressure field.
556 *Journal of Climate* 12, 1070–1085.
- 557 Brauner, N., Shacham, M., 1998. Role of range and precision of the indepen-
558 dent variable in regression of data. *Aiche Journal* 44, 603–611.
- 559 Brotons, L., Thuiller, W., Miguel, B., 2004. Presence-absence versus
560 presence-only modelling methods for predicting bird habitat suitability.
561 *Ecography* 27, 437–448.
- 562 Cano, R., 1999. Atlas climático de la Región Cantábrica. Nota Técnica
563 CMT/CAS. Instituto Nacional de Meteorología. In Spanish.
- 564 Chevan, A., Sutherland, M., 1991. Hierarchical partitioning. *The American*
565 *Statistician* 45, 90–96.

- 566 Christensen, O., Drews, M., Christensen, J., Dethloff, K., Ketelsen, K.,
567 Hebestadt, I., Rinke, A., 2006. The HIRHAM regional climate model ver-
568 sion 5. Technical Report. Danish Meteorological Institute. Copenhagen,
569 Denmark.
- 570 Cohen, J., Cohen, P., West, S.G., Aiken, L.S., 2003. Applied Multiple Regres-
571 sion / Correlation Analysis for the Behavioral Sciences. Lawrence Erlbaum
572 Associates, New Jersey, USA. 3rd edition.
- 573 Collins, M., Booth, B., Harris, G., Murphy, J., Sexton, D., M., W., 2006.
574 Towards quantifying uncertainty in transient climate change. *Climate Dy-*
575 *namics* 27, 127–147.
- 576 Costa, M., Morla, C., Sainz, H., 1998. Los bosques ibéricos. Una inter-
577 pretación geobotánica. Planeta, Barcelona, Spain. In spanish.
- 578 Elith, J., Graham, C.H., Anderson, R.P., Dudik, M., Ferrier, S., Guisan,
579 A., Hijmans, R.J., Huettmann, F., Leathwick, J.R., Lehmann, A., Li, J.,
580 Lohmann, L.G., Loiselle, B.A., Manion, G., Moritz, C., Nakamura, M.,
581 Nakazawa, Y., Overton, J.M., Peterson, A.T., Phillips, S.J., Richardson,
582 K., Scachetti-Pereira, R., Schapire, R.E., Soberon, J., Williams, S., Wisz,
583 M.S., Zimmermann, N.E., 2006. Novel methods improve prediction of
584 species' distributions from occurrence data. *Ecography* 29, 129–151.
- 585 Elith, J., Leathwick, J.R., 2009. Species distribution models: Ecological ex-
586 planation and prediction across space and time. *Annual Review of Ecology*
587 *Evolution and Systematics* 40, 677–697.

- 588 Felicísimo, A.M., Muñoz, J., Villalba, C.J., Mateo, R.G., 2010. Impactos,
589 vulnerabilidad y adaptación al cambio climático de la flora española. Tech-
590 nical Report. Universidad de Extremadura, Real Jardín Botánico (CSIC),
591 Oficina Española de Cambio Climático. In Spanish.
- 592 Franklin, J., Davis, F., Ikegami, M., Syphard, A., Flint, L., Flint, A., Han-
593 nah, L., 2013. Modeling plant species distributions under future climates:
594 how fine scale do climate projections need to be? *Global Change Biology*
595 19, 473–483.
- 596 Friedman, J.H., 1991. Multivariate adaptive regression splines. *Annals of*
597 *Statistics* 19, 1–67.
- 598 Fronzek, S., Carter, T., Luoto, M., 2011. Evaluating sources of uncertainty
599 in modelling the impact of probabilistic climate change on sub-arctic palsa
600 mires. *Natural Hazards and Earth System Sciences* 11, 2981–2995.
- 601 Graham, C.H., Elith, J., Hijmans, R.J., Guisan, A., Peterson, A.T., Loiselle,
602 B.A., The NCEAS Predicting Species Distributions Working Group, 2008.
603 The influence of spatial errors in species occurrence data used in distribu-
604 tion models. *Journal of Applied Ecology* 45, 239–247.
- 605 Graham, M., 2003. Confronting multicollinearity in ecological multiple re-
606 gression. *Ecology* 84, 2809–2815.
- 607 Guisan, A., Edwards, T.C., Hastie, T., 2002. Generalized linear and general-
608 ized additive models in studies of species distributions: setting the scene.
609 *Ecological Modelling* 157, 89–100.

- 610 Guisan, A., Zimmermann, N.E., 2000. Predictive habitat distribution models
611 in ecology. *Ecological Modelling* 135, 147–186.
- 612 Gutiérrez, J.M., Herrera, S., San Martín, D., Sordo, C., Rodríguez, J.J., Fro-
613 choso, M., Ancell, R., Fernández, J., Cofiño, A.S., Pons, M.R., Rodríguez,
614 M.A., 2010. Escenarios Regionales Probabilísticos de cambio climático
615 en Cantabria: Termopluviometría. Gobierno de Cantabria-Consejería de
616 Medio Ambiente y Universidad de Cantabria, Santander, Spain. In Span-
617 ish.
- 618 Haylock, M.R., Hofstra, N., Klein-Tank, A.M.G., Klok, E.J., Jones, P.D.,
619 New, M., 2008. A European daily high-resolution gridded data set of sur-
620 face temperature and precipitation for 1950-2006. *Journal of Geophysical*
621 *Research* 113.
- 622 Hengl, T., Heuvelink, G., Rossiter, D., 2007. About regression-kriging: From
623 equations to case studies. *Computers and Geosciences* 33, 1301–1315.
- 624 Hijmans, R.J., Cameron, S.E., Parra, J.L., Jones, P.G., Jarvis, A., 2005.
625 Very high resolution interpolated climate surfaces for global land areas.
626 *International Journal of Climatology* 25, 1965–1978.
- 627 Hijmans, R.J., Graham, C.H., 2006. The ability of climate envelope models
628 to predict the effect of climate change on species distributions. *Global*
629 *Change Biology* 12, 2272–2281.
- 630 Hijmans, R.J., Phillips, S., Leathwick, J., Elith, J., 2012. *dismo*: Species
631 distribution modeling. R package version 0.7-23.

632 Jacob, D., Barring, L., Christensen, O.B., Christensen, J.H., de Castro, M.,
633 Deque, M., Giorgi, F., Hagemann, S., Lenderink, G., Rockel, B., Sanchez,
634 E., Schaer, C., Seneviratne, S.I., Somot, S., van Ulden, A., van den Hurk,
635 B., 2007. An inter-comparison of regional climate models for Europe:
636 model performance in present-day climate. *Climatic Change* 81, 31–52.

637 Jacob, D., Van den Hurk, B., Andrae, U., Elgered, G., Fortelius, C., Graham,
638 L., Jackson, S., Karstens, U., Kopken, C., Lindau, R., Podzun, R., Rockel,
639 B., Rubel, F., Sass, B., Smith, R., Yang, X., 2001. A comprehensive
640 model inter-comparison study investigating the water budget during the
641 BALTEX–PIDCAP period. *Meteorology and Atmospheric Physics* 77, 19–
642 43.

643 Jeschke, J.M., Strayer, D.L., 2008. Usefulness of bioclimatic models for study-
644 ing climate change and invasive species, in: *YEAR IN ECOLOGY AND*
645 *CONSERVATION BIOLOGY 2008*. BLACKWELL PUBLISHING, 9600
646 GARSINGTON RD, OXFORD OX4 2DQ, OXEN, ENGLAND. volume
647 1134 of *ANNALS OF THE NEW YORK ACADEMY OF SCIENCES*,
648 pp. 1–24.

649 Juang, K., Lee, D., 1998. Simple indicator kriging for estimating the prob-
650 ability of incorrectly delineating hazardous areas in a contaminated site.
651 *Environmental Science & Technology* 32, 2487–2493.

652 Khaliq, M.N., Ouarda, T.B.M.J., 2007. On the critical values of the Standard
653 Normal Homogeneity Test (SNHT). *International Journal of Climatology*
654 27, 681–687.

- 655 Kjellström, E., Barring, L., Gollvik, S., Hansson, U., Jones, C., Samuelsson,
656 P., Rummukainen, M., Ullerstig, A., Willén, U., Wyser, K., 2005. A 140–
657 year simulation of European climate with the new version of the Rossby
658 Centre regional atmospheric climate model (RCA3). Rep. Meteorol. Cli-
659 matol. 108, 681–687.
- 660 Kramer, K., Degen, B., Buchsbom, J., Hickler, T., Thuiller, W., Sykes, M.T.,
661 de Winter, W., 2010. Modelling exploration of the future of European
662 beech (*Fagus sylvatica* L.) under climate change - Range, abundance, ge-
663 netic diversity and adaptive response. Forest Ecology and Management
664 259, 2213–2222.
- 665 Krige, D.G., 1951. A statistical approach to some basic mine valuation prob-
666 lems on the Witwatersrand. Journal of the Chemical, Metallurgical and
667 Mining Society of South Africa 52, 119–139.
- 668 Kriticos, D.J., Webber, B.L., Leriche, A., Ota, N., Macadam, I., Bathols, J.,
669 Scott, J.K., 2012. Climond: global high-resolution historical and future
670 scenario climate surfaces for bioclimatic modelling. Methods in Ecology
671 and Evolution 3, 53–64.
- 672 Landis, J., Koch, G., 1977. Measurement of observer agreement for categor-
673 ical data. Biometrics 33, 159–174.
- 674 MARM, 2006. Tercer inventario forestal nacional.
- 675 Mateo, R.G., Croat, T.B., Felicísimo, A.M., Muñoz, J., 2010. Profile or group
676 discriminative techniques? Generating reliable species distribution mod-

- 677 els using pseudo-absences and target-group absences from natural history
678 collections. *Diversity and Distributions* 16, 84–94.
- 679 McPherson, J.M., Jetz, W., Rogers, D.J., 2004. The effects of species range
680 sizes on the accuracy of distribution models: ecological phenomenon or
681 statistical artefact? *Journal of Applied Ecology* 41, 811–823.
- 682 Murray, K., Conner, M., 2009. Methods to quantify variable importance:
683 implications for the analysis of noisy ecological data. *Ecology* 90, 348–355.
- 684 Nakićenović, N., 2000. Greenhouse Gas Emissions Scenarios. *Technological*
685 *Forecasting and Social Change* 65, 149–166.
- 686 Ninyerola, M., Pons, X., Roure, J.M., 2005. Atlas climático digital de
687 la Península Ibérica. Metodología y aplicaciones en bioclimatología y
688 geobotánica. Universitat Autònoma de Barcelona, Cerdanyola del Vallès,
689 Spain. In Spanish.
- 690 Pal, J.S., Giorgi, F., Bi, X., Elguindi, N., Solmon, F., Gao, X., Rauscher,
691 S.A., Francisco, R., Zakey, A., Winter, J., Ashfaq, M., Syed, F.S., Bell,
692 J.L., Diffenbaugh, N.S., Karmacharya, J., Konare, A., Martínez, D.,
693 da Rocha, R.P., Sloan, L.C., Steiner, A.L., 2007. Regional climate model-
694 ing for the developing world: The ICTP RegCM3 and RegCNET. *Bulletin*
695 *of the American Meteorological Society* 88, 1395–1409.
- 696 Peterson, A., Ortega-Huerta, M., Bartley, J., Sánchez-Cordero, V., Soberón,
697 J., Buddemeier, R., Stockwell, D., 2002. Future projections for mexican
698 faunas under global climate change scenarios. *Letters to Nature* 416, 626–
699 629.

- 700 Peterson, A.T., Nakazawa, Y., 2008. Environmental data sets matter in eco-
701 logical niche modelling: an example with *Solenopsis invicta* and *Solenopsis*
702 *richteri*. *Global Ecology and Biogeography* 17, 135–144.
- 703 R Development Core Team, 2012. R: A Language and Environment for
704 Statistical Computing. R Foundation for Statistical Computing. ISBN
705 3-900051-07-0.
- 706 Radu, R., Déqué, M., Somot, S., 2008. Spectral nudging in a spectral regional
707 climate model. *Tellus A* 60, 898–910.
- 708 Räisänen, J., 2007. How reliable are climate models? *Tellus A* 59, 2–29.
- 709 Randin, C.F., Engler, R., Normand, S., Zappa, M., Zimmermann, N.E.,
710 Pearman, P.B., Vittoz, P., Thuiller, W., Guisan, A., 2009. Climate change
711 and plant distribution: local models predict high-elevation persistence.
712 *Global Change Biology* 15, 1557–1569.
- 713 Soria-Auza, R.W., Kessler, M., Bach, K., Barajas-Barbosa, P.M., Lehnert,
714 M., Herzog, S.K., Böner, J., 2010. Impact of the quality of climate models
715 for modelling species occurrences in countries with poor climatic documen-
716 tation: a case study from Bolivia. *Ecological Modelling* 221, 1221–1229.
- 717 Swets, J., 1988. Measuring the accuracy of diagnostic systems. *Science* 240,
718 1285–1293.
- 719 Tadić, M.P., 2010. Gridded croatian climatology for 1961-1990. *Theoretical*
720 *and Applied Climatology* 102, 87–103.

- 721 Thuiller, W., 2003. BIOMOD - Optimizing predictions of species distribu-
722 tions and projecting potential future shifts under global change. *Glob.*
723 *Change Biol.* 9, 1353–1362.
- 724 Tsoar, A., Allouche, O., Steinitz, O., Rotem, D., Kadmon, R., 2007. A com-
725 parative evaluation of presence-only methods for modelling species distri-
726 bution. *Diversity and Distributions* 13, 397–405.
- 727 van der Linden, P., Mitchell, J., 2009. ENSEMBLES: Climate change and its
728 impacts: Summary of research and results from the ENSEMBLES project.
729 Technical Report. Met Office Hadley Centre. Exeter, UK.
- 730 van Meijgaard, E., van Ulft, L., van de Berg, W., Bosveld, F., van den Hurk,
731 B., Lenderink, G., Siebesma, A., 2008. The KNMI regional atmospheric
732 climate model RACMO, version 2.1. Tech. Rep. 302. R. Neth. Meteorol.
733 Inst.. De Bilt, Netherlands.
- 734 Wiens, J.A., Stralberg, D., Jongsomjit, D., Howell, C.A., Snyder, M.A.,
735 2009. Niches, models, and climate change: Assessing the assumptions
736 and uncertainties. *PROCEEDINGS OF THE NATIONAL ACADEMY*
737 *OF SCIENCES OF THE UNITED STATES OF AMERICA* 106, 19729–
738 19736. Arthur M Sackler Colloquium of the National-Academy-of-Sciences
739 on Biogeography, Changing Climates and Niche Evolution, Irvine, CA,
740 DEC 12-13, 2008.
- 741 Wilting, A., Cord, A., Hearn, A.J., Hesse, D., Mohamed, A., Traeholdt,
742 C., Cheyne, S.M., Sunarto, S., Jayasilan, M.A., Ross, J., Shapiro, A.C.,
743 Sebastian, A., Dech, S., Breitenmoser, C., Sanderson, J., Duckworth, J.W.,

- 744 Hofer, H., 2010. Modelling the Species Distribution of Flat-Headed Cats
745 (Prionailurus planiceps), an Endangered South-East Asian Small Felid.
746 PLOS ONE 5.
- 747 Winkler, J.A., Palutikof, J.P., Andresen, J.A., Goodess, C.M., 1997. The
748 Simulation of Daily Temperature Time Series from GCM Output. Part
749 II: Sensitivity Analysis of an Empirical Transfer Function Methodology.
750 Journal of Climate 10, 2514–2532.
- 751 Yamamoto, J.K., 2000. An alternative measure of the reliability of ordinary
752 kriging estimates. Mathematical Geology 32, 489–509.
- 753 Zahn, M., von Storch, H., 2010. Decreased frequency of North Atlantic polar
754 lows associated with future climate warming. Nature 467, 309–312.

Code	Variable definition	units	Mean	UAB error			WC error		
				<i>RMSE</i>	<i>rho</i>	<i>Bias</i>	<i>RMSE</i>	<i>rho</i>	<i>Bias</i>
BIO1	Mean annual temp.	$^{\circ}C$	10.64	0.49	0.97	0.05	0.47	0.97	0.12
BIO2	Mean diurnal temp. range	$^{\circ}C$	11.5	1.22	0.76	0.60	3.13	0.82	2.99
BIO3	Isothermality (BIO2/BIO7) \times 100	%	44.53	2.24	0.43	-0.85	6.37	-0.20	-6.01
BIO4	Temp. seasonality ($\sigma \times 100$)	%	521.51	28.54	0.96	-11.87	44.7	0.95	29.05
BIO5	Max. temp. of warmest month	$^{\circ}C$	25.31	1.07	0.85	-0.4	2.6	0.77	-2.34
BIO6	Min. temp. of coldest month	$^{\circ}C$	-0.53	0.97	0.96	0.42	1.61	0.97	1.47
BIO7	Annual temp. range	$^{\circ}C$	25.84	1.74	0.94	-0.82	4.09	0.94	-3.81
BIO8	Mean temp. of wettest quarter	$^{\circ}C$	5.66	1.36	0.90	0.28	2.72	0.83	2.3
BIO9	Mean temp. of driest quarter	$^{\circ}C$	17.15	0.54	0.91	-0.05	0.8	0.88	-0.50
BIO10	Mean temp. of warmest quarter	$^{\circ}C$	17.26	0.53	0.92	-0.07	0.72	0.91	-0.41
BIO11	Mean temp. of coldest quarter	$^{\circ}C$	4.59	0.64	0.97	0.24	0.64	0.96	0.22
BIO12	Annual precip.	<i>mm</i>	1015.8	173.12	0.91	44.28	339.12	0.73	-130.69
BIO13	Precip. of wettest month	<i>mm</i>	128.38	22.71	0.92	-3.13	44.81	0.81	-22.72
BIO14	Precip. of driest month	<i>mm</i>	38.28	9.37	0.91	6.6	13.65	0.64	4.13
BIO15	Seasonality of precip.(<i>cv</i> \times 100)	%	33.97	4.84	0.66	-3.42	10.79	0.15	-9.45
BIO16	Precip. of wettest quarter	<i>mm</i>	353.33	61.81	0.92	0.82	124.51	0.79	-63.51
BIO17	Precip. of driest quarter	<i>mm</i>	136.3	28.73	0.91	20.08	44.19	0.69	20.43
BIO18	Precip. of warmest quarter	<i>mm</i>	144.12	26.84	0.91	15.67	47.21	0.79	22.44
BIO19	Precip. of coldest quarter	<i>mm</i>	317.43	58.69	0.91	4.87	123.96	0.65	-68.2

Table 1: Summary of explanatory bioclimatic variables used for climate envelope models. The spatial mean values computed with the reference climatology (UC) are indicated in the fourth column. Errors of the other two climate datasets (UAB and WC) w.r.t. UC data are indicated in terms of their root mean square error (RMSE) Spearman’s rho correlation (rho) and bias. σ = standard deviation, *cv* = coefficient of variation.

Institution	Model	boundary GCM	Reference
Centre National de Recherches Météorol.	RM4.5	CNRM-CM3	Radu et al. (2008)
Danish Meteorol. Inst.	HIRHAM5	CNRM-CM3	Christensen et al. (2006)
Koninklijk Nederlands Meteorol. Inst.	RACMO2	MPI-ECHAM5-r3	van Meijgaard et al. (2008)
Hadley Center/UK Met Office	HadRM3	HadCM3-Q0	Collins et al. (2006)
Abdus Salam Int. Centre for Theor. Phys.	RegCM3	HadCM3-Q0	Pal et al. (2007)
Max Planck Inst. for Meteorol.	REMO	MPI-ECHAM5-r3	Jacob et al. (2001)
Swedish Meteorol. and Hydrol. Inst.	RCA3.0	BCCR-BCM2	Kjellström et al. (2005)

Table 2: Summary of the ENSEMBLES regional climate models used in this study. The driving GCMs and related references are also indicated.

Dataset	BIO Variable
UC	9, 16*, 3, 18*, 14*
UAB	5, 2, 14*, 18*, 16*, 15*
WC	9, 5, 2, 14*, 19*

Table 3: Variable subsets resulting after the application of the variable selection procedure (Section 3.3) to each of the climate datasets. Variables are displayed in their order of inclusion in the models. Precipitation-related variables are marked with an asterisk.

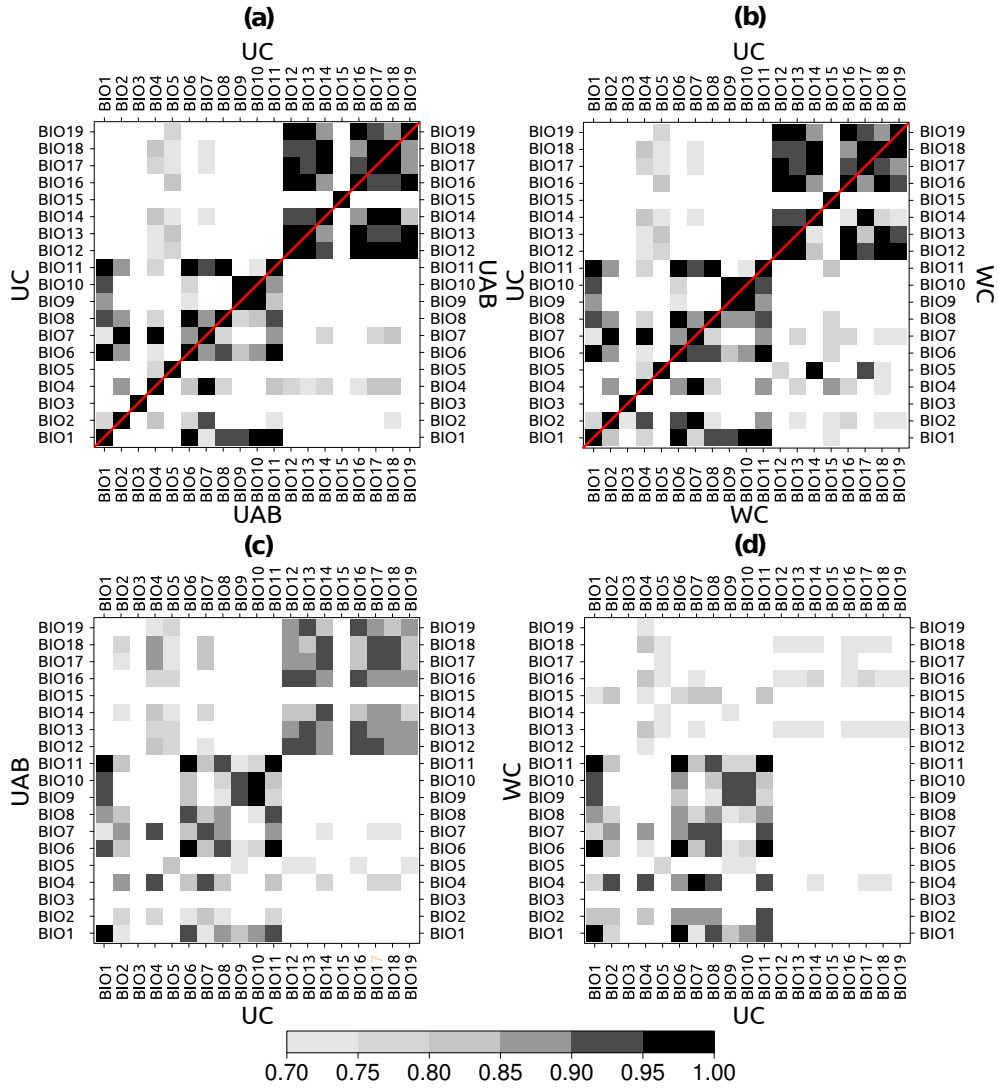


Figure 2: Pairwise cross-correlation matrices of the bioclimatic variables (Spearman's rho correlation coefficients). Values below 0.7 not shown). Intra-dataset correlation matrices (truncated) are displayed in the upper panels for UAB (a) and WC (b). Note that the benchmark UC dataset is represented in both panels (a and b) for better comparability. Inter-dataset correlation matrices are displayed in the lower panels: (c) UAB *vs.* UC and (d) WC *vs.* UC. Note that variables from BIO1 to BIO11 are related with temperature, and from BIO12 to BIO19 with precipitation (see Table 1 for details).

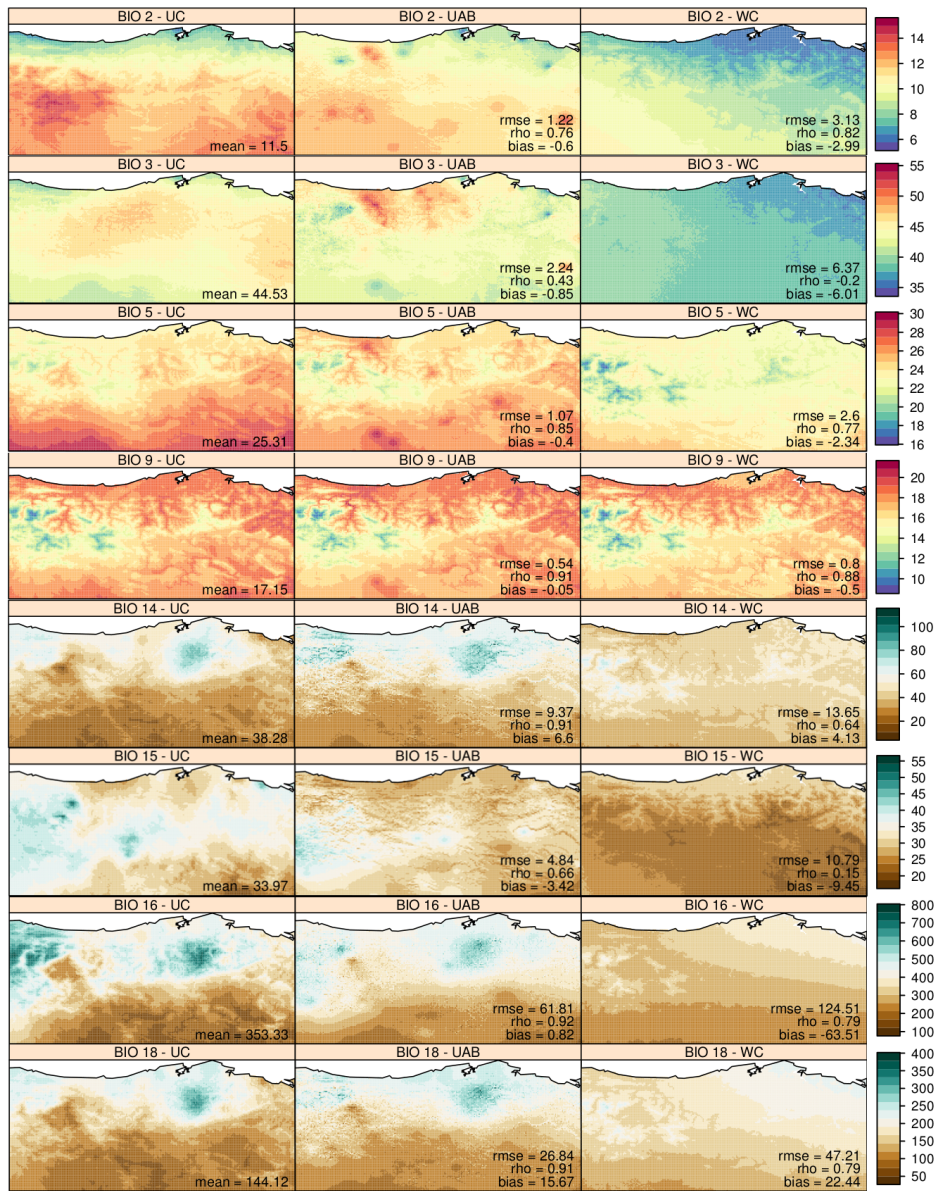


Figure 3: . Bioclimatic variables included in the UC, UAB and WC subsets after the variable selection procedure (Table 3). Mean UC values are indicated in the lower right hand side of the corresponding panels. For UAB and WC, the root mean square error (rmse), Spearman's rho correlation coefficient (rho) and bias with regard to UC are indicated. For details on variable definition and units see Table 1.

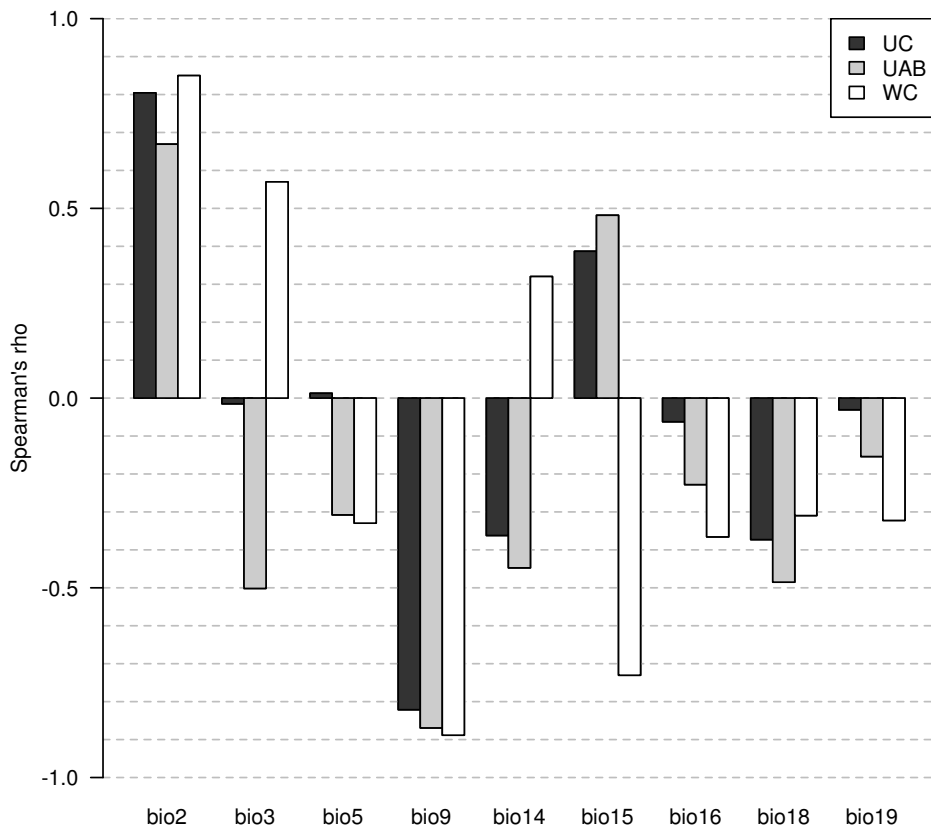


Figure 4: Correlation coefficients of the bioclimatic variables used in the different models with the terrain elevation, according to the three datasets tested.

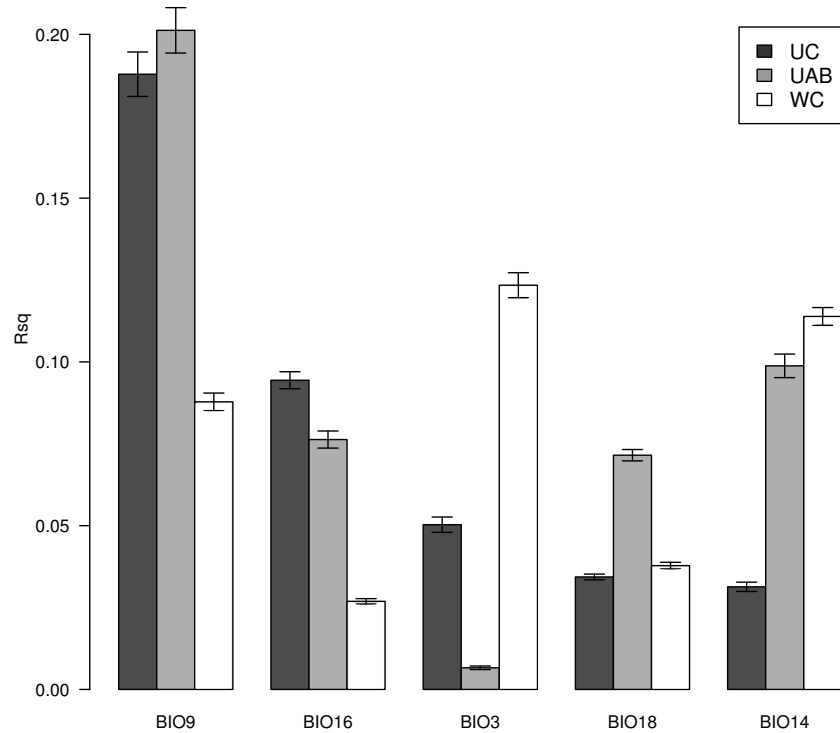


Figure 5: Variable importance (R^2) estimated as the independent effect of each variable following the hierarchical partitioning approach (Section 3.4). Variables selected correspond to the UC model selection. Values represented correspond to the mean \pm standard deviation of the $k=10$ models of the cross validation test.

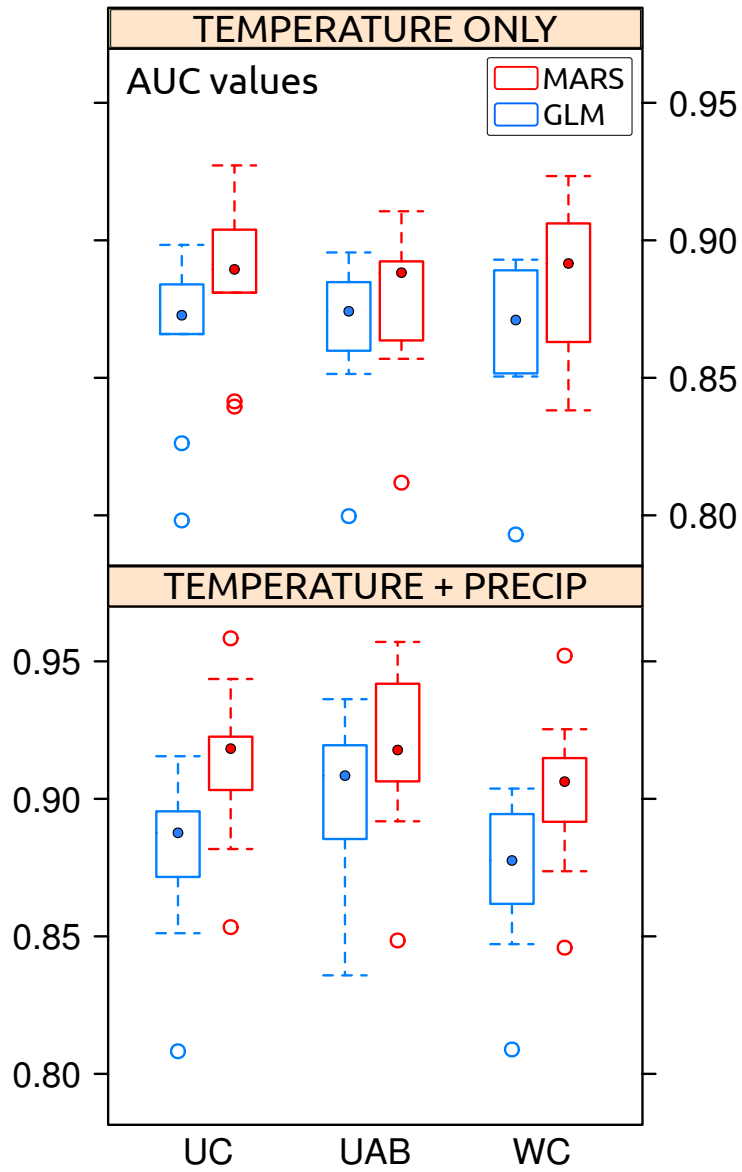


Figure 6: Area under the ROC curve (AUC) attained by the different CEMs in the 10-fold cross validation. The results are shown for both the temperature-only models, and for the temperature and precipitation models (using the variable subsets indicated in Table 3). The results are presented for both the GLM and the MARS algorithms.

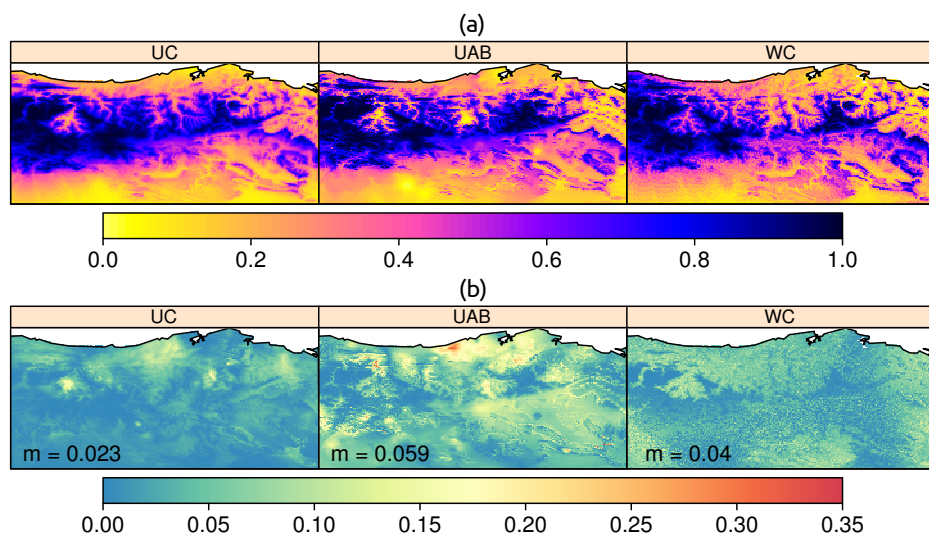


Figure 7: (a): Distribution maps obtained for *Fagus* according to the three datasets tested, using each one its corresponding subset of predictor variables (Table 3). (b): Multi predictor dataset uncertainty (standard deviation units) of the above models (spatial mean (m) is indicated for each panel).

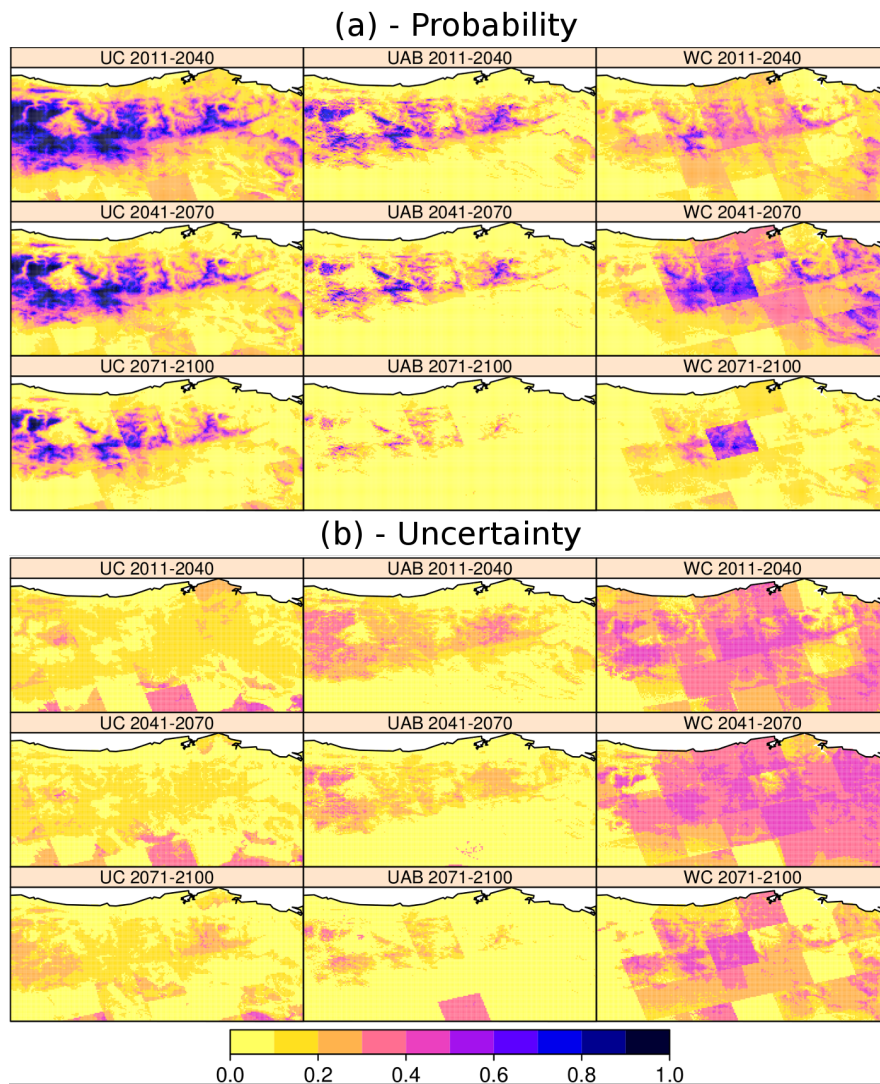


Figure 8: CEM future projections calculated according to the UC, UAB and WC climate datasets, using their respective subsets of predictors (Table 3). Maps in (a) represent the multi-RCM ensemble projections (Table 2) for the three future transient periods considered. Maps in (b) represent the standard deviation of the multi-model ensemble means.